Structure study of ^{40}Ca by α+^{36}Ar cluster model

Toshimi Sakuda
Department of Physics, Miyazaki University, Miyazaki 889-21, Japan

Shigeo Ohkubo
Department of Applied Science, Kochi Women's University, Kochi 780, Japan
and Nuclear Physics Laboratory, University of Oxford, Oxford OX1 3RH, United Kingdom
(Received 15 June 1993)

The energy spectra, α-spectroscopic factors, and $E2$ transitions of ^{40}Ca are studied by the α+^{36}Ar orthogonality condition model. The calculated properties are in good overall agreement with the experimental data. Both of the $K=0^+$ and 0^- cluster bands are successfully reproduced by the model. It is found that the coexistence and interference of α-cluster states and shell-model states are important for understanding the structure of ^{40}Ca.

PACS number(s): 21.60.Gx, 27.40.+z

I. INTRODUCTION

Recent developments [1–7] have revived the interest for cluster structure in fp-shell nuclei. In the ^{44}Ti nucleus, both the $K=0^+$ and 0^- α+^{40}Ca cluster bands have been convincingly identified by the α-transfer experiments [8–10]. More recently, the α-transfer reaction leading to ^{40}Ca has also been carried out [11] and has disclosed the presence of the parity doublet of the α+^{36}Ar cluster bands, which is quite similar to that of ^{44}Ti. These observations strongly suggest that the α-cluster structure may persist throughout the fp-shell region. There has been a large amount of experimental data on ^{40}Ca. The ^{40}Ca nucleus should provide a good testing ground for studying this persistence.

The structure of the ^{40}Ca nucleus is characterized by the coexistence of the spherical shell-model configuration and multiparticle-multihole deformed configurations. Therefore, we should incorporate these configurations in order to investigate the real existence of the α-cluster states in ^{40}Ca.

We employ the microscopic α+^{36}Ar orthogonality condition model (OCM) for the present study of ^{40}Ca. This model is a sort of unified model, because it can describe simultaneously cluster states and important shell-model states. The OCM was applied to the ^{40}Ca system by Ogawa, Suzuki, and Ikeda [12]. They found a $K=0^+$ band with an α+^{36}Ar cluster structure more or less, but could not obtain a $K=0^-$ cluster band. They concluded that shell structure is predominant and typical cluster states are hardly observed in low-lying levels of ^{40}Ca. We would like to propose an alternative parametrization of the intercluster potential derived from more realistic two-nucleon interaction, which predicts a $K=0^-$ cluster band as well as $K=0^+$ one. Furthermore, we also investigate to what degree the model reproduces the data of the α-spectroscopic factors and electric transitions.

II. ORTHOGONALITY CONDITION MODEL FOR α+^{36}Ar SYSTEM

The model space is spanned by the wave functions

$$\frac{\mathcal{A}}{\sqrt{\binom{40}{4}}}\{\phi(\alpha)\,[\,\phi_L(^{36}\mathrm{Ar})\,Y_l(\hat{\mathbf{r}})\,]_J\,R_{Nl}(r)\}\,, \qquad (1)$$

where $R_{Nl}(r)$ is a radial harmonic oscillator wave function with N oscillator quanta of the relative motion. The internal wave functions $\phi(\alpha)$ and $\phi_L(^{36}\mathrm{Ar})$ are assumed to be $(0s)^4$ and $(sd)^{-4}(\lambda\mu)=(08)$ configurations, respectively, with a common oscillator parameter a=0.2815 fm^{-2}. We make a truncation of the model space: the total oscillator quanta N=8–30 and the relative angular momentum l=0–20. We generate the model space as a product of the internal wave functions and the relative ones: $(N0)\times(08)=(N,8)+(N-1,7)+(N-2,6)+\cdots+(N-8,0)$. Therefore, the states forbidden by the Pauli principle can be completely removed. The present model space includes important shell-model states such as the sd-closed $(\lambda,\mu)=(0,0)$ configuration, the (2,1) and (3,2) of 1p-1h (one-particle–one-hole) states, and the (12,8) of 4p-4h states.

The Hamiltonian of the system is given by

$$H=H(\alpha)+H(^{36}\mathrm{Ar})+T_r+V_{\alpha\text{-Ar}}\,. \qquad (2)$$

The excitation energies of ^{36}Ar are taken from the experiments and the values used in Ref. [12]. The intercluster potential $V_{\alpha\text{-Ar}}$ is obtained by double folding a two-nucleon interaction and the Coulomb interaction, and can be expressed in operator form [13] as

$$V_{\alpha\text{-Ar}}=V^C+V^L\boldsymbol{L}^2+V^{T2}\,[T_2,Y_2]_0+V^{T2'}\,[T_2',Y_2]_0 +V^{T4}\,[T_4,Y_4]_0\,, \qquad (3)$$

where

$$T_{\lambda\mu} = \sum_{i\in \mathrm{Ar}} y_{\lambda\mu}(\boldsymbol{\xi}_i) \ , \qquad T'_{2\mu} = \sum_{i\in \mathrm{Ar}} \xi_i^2 y_{2\mu}(\boldsymbol{\xi}_i) \ , \qquad (4)$$

and L is the angular momentum of ^{36}Ar. The underlying two-nucleon interaction is Hasegawa-Nagata-Yamamoto force [14] with the depth parameter $V_0(^3E) = -490$ MeV for the intermediate range, which is similar to the value used successfully in the ^{44}Ti system [2,15]. Among the noncentral parts of the folding potential, the T_2 and T'_2 terms are found to be dominant coupling potentials and the others are very small. The depths V^{T2} and $V^{T2'}$ are multiplied by factors 1.35 and 0.65, respectively, so as to give a good agreement for low-lying states energies.

A. Energy spectra

The calculated and experimental energy spectra are shown in Fig. 1, where energies are measured from the α+^{36}Ar threshold ($E_{\mathrm{th}} = 7.04$ MeV). The experimental levels marked by an asterisk are strongly populated in the α-transfer reactions [11,16]. In the calculated spectra, the members of the predominantly α+^{36}Ar(0^+) cluster band are also marked by an asterisk. Our calculations are found to be in good agreement with both of the experimental K=0^+ and K=0^- cluster bands. This result disagrees with the result of Ref. [12]. The discrepancy is probably due to the differences of the two-nucleon interactions and the adjustment of the folding potential.

The dominantly weak coupling ^{36}Ar(2^+)$\times l$ band is predicted to lie on the 2^+_2 state in the present calculation. The observed 2^+_2($E_x = 5.25$ MeV), 3^+_1($E_x = 6.02$ MeV), and 4^+_2($E_x = 6.51$ MeV) states, which are commonly interpreted as 4p-4h K=2^+ band, are good candidates for the members. This identification differs from that of Ref. [6]. A further support to our interpretation is provided by the $E2$ transitions of the levels. In order to identify candidates to the other members of weak coupling multiplet, qualitative data on the levels at around the α-threshold is needed. The observed 0^+_3($E_x = 5.21$ MeV), 2^+_3($E_x = 5.63$ MeV), and 4^+_3($E_x = 6.54$ MeV) states are usually classified as the 8p-8h band [17,18], which are outside the framework of the present model. The low-lying negative-parity states are dominantly mixtures of 1p-1h and 3p-3h configurations and are reasonably reproduced within the present model. Some differences of ordering of the levels might be resolved, if we take account of the spin-orbit splittings of single-particle states.

B. Wave functions and α-spectroscopic factors

The calculated wave functions and α-spectroscopic factors of α+^{36}Ar(0^+) channel for the K=0^+ and 0^- cluster bands are given in Table I. The ground state 0^+_1 is shown to have a dominant (93%) closed shell component. The K=0^+ band is largely of the α-cluster nature and contains rather few N=8 and 10 components. It can be seen that the mixture of the N=11 component in the K=0^- cluster band is considerably larger than the mixture of

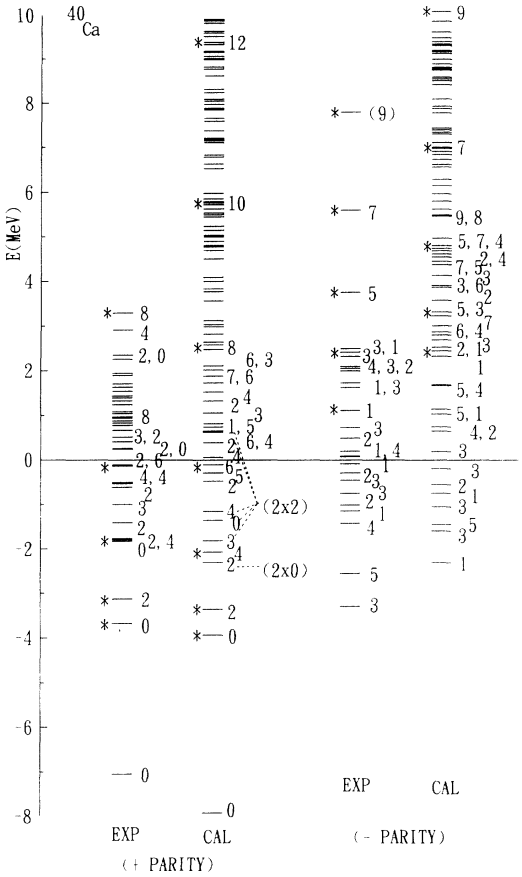

FIG. 1. Calculated and experimental energy spectra of ^{40}Ca. The energy scale is measured from the α threshold. The states marked by an asterisk are the members of α+^{36}Ar cluster bands. The multiplets of weak coupling ^{36}Ar(2^+)$\times l$ band are indicated by dotted lines. Experimental energies are from Refs. [11,21].

TABLE I. α-spectroscopic factors and squared components with N oscillator quanta of the wave functions for the K=0^+ and 0^- cluster bands. Those of the ground 0^+ state are also presented for comparison. Experimental values are from Ref. [11].

J^π	E (MeV)		S^2_α		N		
	CAL	EXP	CAL	EXP	8	10	12
0^+_{gr}	-7.93	-7.04(0.00)	0.086	0.30	0.933	0.031	0.033
0^+	-3.94	-3.69(3.35)	0.194	0.21	0.000	0.033	0.585
2^+	-3.36	-3.14(3.90)	0.177	0.26		0.021	0.603
4^+	-2.06	-1.76(5.27)	0.142	0.19		0.009	0.629
6^+	-0.10	-0.11(6.93)	0.101	0.25		0.003	0.653
8^+	2.47	3.30(10.34)	0.063	0.25		0.004	0.672
10^+	5.63		0.041			0.002	0.715
12^+	9.18		0.035				0.924
					9	11	13
1^-	2.45	1.11 (8.15)	0.156	0.21	0.027	0.146	0.353
3^-	3.32	2.66 (9.70)	0.153	0.20	0.007	0.139	0.371
5^-	4.82	3.76(10.80)	0.125	0.14	0.001	0.131	0.382
7^-	6.92	5.61(12.65)	0.094	0.11		0.110	0.394
9^-	10.92	7.81(14.85)	0.095	0.33		0.060	0.522
11^-	14.55		0.057			0.037	0.537

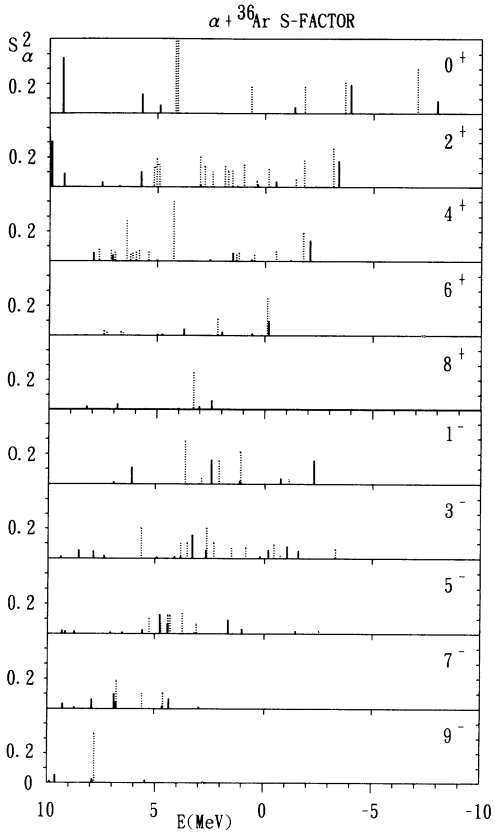

FIG. 2. Calculated (solid line) and experimental (dashed line) α-spectroscopic factors of ^{40}Ca. Experimental values are from Ref. [11].

the N=10 component in the K=0$^+$ band. This is responsible for the result that the K=0$^-$ band has, on the average, smaller S_α^2 factors than the K=0$^+$ band. It is surprising that the coupling between shell-model states and cluster states becomes stronger in the negative-parity states rather than in the positive-parity states. A difference in situations of the unperturbed energies is responsible for this feature of configuration mixing. In the positive-parity states, the 2p-2h states are expected to occur at the energies higher than those of the α-cluster states. On the other hand, in the negative parity states the 1p-1h and 3p-3h states occur at lower or about the same energy region as the α-cluster states, which leads to more mixing between them.

In Fig. 2, all of the calculated S_α^2 factors of the $\alpha+^{36}$Ar(0$^+$) channel are compared with the experimental values. Characteristically, the α-cluster strength is shared over many levels and some levels, other than α-cluster levels, possess appreciable S_α^2 factors. We can, however, identify the cluster states which have noticeably large S_α^2 factors. Gross properties of the distribution of the α-cluster strength are consistently explained within the present model. The extremely large peaks with $J^\pi = 0^+, 2^+$, and 4^+ around $E \approx 5$ MeV can be understood to correspond to the higher nodal states. The calculated higher nodal states are about 5 MeV higher than the experimental ones. This discrepancy is probably due to the bound-state description of the higher nodal states.

A decomposition of the wave functions into channel components would be interesting. The spectroscopic factors S_α^2 of the $\alpha+^{36}$Ar ($L^\pi = 0^+, 2^+, 4^+$) channels for the positive parity states are listed in Table II. The

TABLE II. Spectroscopic factors S_α^2 of the $\alpha+^{36}$Ar ($L^\pi = 0^+, 2^+, 4^+$) channels for the positive parity states.

J_i^π	Channel ($L \times l$)								
	(0× 0)	(2×2)			(4×4)				
0_1^+	0.086	0.427			0.765				
0_2^+	0.194	0.030			0.003				
0_3^+	0.043	0.186			0.025				
		(2×2)			(4×4)				
1_1^+		0.259			0.020				
	(0×2)	(2×0)	(2×2)	(2×4)	(4×2)	(4×4)	(4×6)		
2_1^+	0.177	0.016	0.014	0.009	0.002	0.001	0.001		
2_2^+	0.001	0.112	0.094	0.001	0.003	0.004	0.000		
2_3^+	0.036	0.013	0.029	0.100	0.016	0.004	0.024		
		(2×2)	(2×4)		(4×2)	(4×4)	(4×6)		
3_1^+		0.181	0.020		0.008	0.002	0.001		
	(0×4)	(2×2)	(2×4)	(2×6)	(4×0)	(4×2)	(4×4)	(4×6)	(4×8)
4_1^+	0.142	0.042	0.013	0.005	0.003	0.002	0.001	0.000	0.001
4_2^+	0.005	0.094	0.094	0.001	0.009	0.001	0.002	0.002	0.000
	(0×6)	(2×4)	(2×6)	(2×8)	(4×2)	(4×4)	(4×6)	(4×8)	(4×10)
6_1^+	0.101	0.066	0.011	0.003	0.012	0.003	0.001	0.000	0.000
6_2^+	0.016	0.072	0.078	0.001	0.023	0.000	0.004	0.001	0.000
	(0×8)	(2×6)	(2×8)	(2×10)	(4×4)	(4×6)	(4×8)	(4×10)	(4×12)
8_1^+	0.063	0.074	0.008	0.002	0.033	0.003	0.001	0.000	0.000
8_2^+	0.024	0.037	0.062	0.001	0.039	0.001	0.005	0.001	0.000

TABLE III. Spectroscopic factors S_α^2 of the α+^{36}Ar ($L^\pi = 0^+, 2^+, 4^+$) channels for the negative parity states.

J_i^π	Channel ($L \times l$)								
	(0×1)	(2×1)	(2×3)		(4×3)	(4×5)			
1_1^-	0.152	0.005	0.029		0.010	0.014			
1_2^-	0.033	0.023	0.045		0.009	0.044			
1_3^-	0.014	0.148	0.021		0.083	0.009			
1_4^-	0.007	0.137	0.022		0.075	0.006			
1_5^-	0.156	0.038	0.102		0.025	0.016			
	(0×3)	(2×1)	(2×3)	(2×5)	(4×1)	(4×3)	(4×5)	(4×7)	
3_1^-	0.047	0.055	0.037	0.063	0.047	0.036	0.034	0.071	
3_2^-	0.077	0.024	0.001	0.027	0.018	0.009	0.001	0.013	
3_3^-	0.052	0.001	0.008	0.022	0.001	0.001	0.015	0.059	
3_4^-	0.003	0.086	0.023	0.001	0.011	0.005	0.029	0.003	
3_5^-	0.048	0.062	0.107	0.019	0.015	0.003	0.016	0.011	
3_6^-	0.152	0.055	0.022	0.057	0.028	0.012	0.006	0.007	
	(0×5)	(2×3)	(2×5)	(2×7)	(4×1)	(4×3)	(4×5)	(4×7)	(4×9)
5_1^-	0.014	0.029	0.016	0.023	0.016	0.014	0.015	0.017	0.022
5_2^-	0.027	0.100	0.001	0.025	0.002	0.003	0.002	0.000	0.004
5_3^-	0.089	0.035	0.012	0.007	0.001	0.001	0.003	0.028	0.001
5_4^-	0.001	0.002	0.006	0.000	0.117	0.032	0.005	0.001	0.000
5_5^-	0.064	0.007	0.078	0.008	0.010	0.038	0.001	0.021	0.006
5_6^-	0.125	0.087	0.003	0.035	0.050	0.030	0.004	0.001	0.003

ground 0_1^+ state is dominantly a shell-model state and has large values of S_α^2 in all channels. This is due to a nonorthogonality of channel wave functions with low oscillator quanta. States 0_2^+, 2_1^+, 4_1^+, and 6_1^+ are well approximated by a single channel and are α+^{36}Ar(0^+) cluster states. State 8_1^+ is a mixed state of the $(L \times l)$=(0×8) and (2×6) cluster configurations, which is a result of the closeness of the unperturbed energies of these configurations. We can also see that states 2_2^+, 0_3^+, 1_1^+, 2_3^+, 3_1^+, 4_2^+, and 6_2^+ are the members of the α+^{36}Ar(2^+) cluster band. These results give us a confirmation of the weak coupling picture of α+^{36}Ar cluster states.

The spectroscopic factors of the negative parity states are given in Table III. States 1_5^-, 3_6^-, and 5_6^- have the largest values in S_α^2 factor in the $(0 \times l)$ channels and therefore are dominantly α+^{36}Ar(0^+) cluster states. The presence of many states below these cluster states complicate the argument somewhat. State 1_1^- has a large S_α^2 factor in the (0×1) channel. While states 1_3^- and 1_4^- have a large S_α^2 factor in the (2×1) channel. A similar situation holds for the 3^- and 5^- states. Then we can see that the α-cluster strengths are divided between these levels. The mixtures of shell-model states and α-cluster states with negative parity are larger than those between positive parity states. This is an interesting difference between ^{40}Ca and ^{16}O.

Let us discuss further the mixing of shell-model states and cluster states. The calculated wave functions of some 0^+ and 1^- states are shown in Tables IV and V, where

TABLE IV. Wave functions of the three lowest 0^+ states in terms of the SU(3) scheme.

N	(λ, μ)	0_1^+	0_2^+	0_3^+
8	(0,0)	0.966	-0.020	0.023
10	(6,4)	-0.022	-0.158	0.674
	(4,2)	-0.054	-0.079	0.382
	(2,0)	0.167	-0.038	0.178
12	(12,8)	-0.009	-0.729	-0.252
	(10,6)	0.004	0.206	-0.152
	(8,4)	0.012	0.103	-0.272
	(6,2)	0.009	0.034	-0.093
	(4,0)	0.180	0.013	-0.042
14	(14,8)	0.004	0.407	0.126
	(12,6)	-0.003	-0.117	0.094
	(10,4)	-0.008	-0.075	0.219
	(8,2)	-0.019	-0.050	0.189
	(6,0)	0.020	-0.030	0.118

TABLE V. Wave functions of the five lowest 1^- states in terms of the SU(3) scheme.

N	(λ, μ)	1_1^-	1_2^-	1_3^-	1_4^-	1_5^-
9	(3,2)	-0.420	-0.835	-0.155	0.049	0.095
	(2,1)	0.063	0.126	0.654	0.671	0.136
11	(9,6)	-0.582	0.345	-0.054	0.015	-0.340
	(8,5)	0.053	0.001	-0.403	-0.433	-0.058
	(7,4)	0.297	-0.027	0.028	-0.028	0.155
	(6,3)	-0.040	-0.021	0.270	0.137	0.013
	(5,2)	-0.115	-0.038	0.008	0.005	-0.047
	(4,1)	0.029	0.040	-0.082	-0.057	-0.012
	(3,0)	-0.000	-0.053	-0.019	-0.021	0.014
13	(13,8)	-0.196	0.154	-0.001	-0.134	0.583
	(12,7)	-0.025	0.007	0.153	0.206	0.070
	(11,6)	0.315	-0.184	0.024	0.010	0.062
	(10,5)	-0.037	0.003	0.243	0.260	0.039
	(9,4)	-0.133	0.016	-0.006	0.006	-0.040
	(8,3)	0.020	0.007	-0.127	-0.075	-0.011
	(7,2)	0.121	0.148	0.012	-0.011	-0.005
	(6,1)	-0.001	0.006	0.183	-0.109	-0.024
	(5,0)	-0.074	-0.113	0.067	-0.057	-0.002
15	(15,8)	0.133	-0.107	-0.007	0.086	-0.435
	(14,7)	0.008	0.001	-0.111	-0.156	-0.025
	(13,6)	-0.231	0.138	-0.016	-0.007	-0.041
	(12,5)	0.014	0.005	-0.190	-0.206	-0.040
	(11,4)	0.160	-0.040	-0.002	-0.021	0.059
	(10,3)	-0.011	-0.009	0.155	0.106	0.022
	(9,2)	-0.092	-0.020	0.020	0.015	-0.027
	(8,1)	0.008	0.012	-0.088	-0.031	-0.009
	(7,0)	0.034	0.008	-0.033	-0.006	0.007

the listed numbers are the coefficients of the SU(3) bases and the components of quanta higher than N=15 are abbreviated. It is seen that the ground 0_1^+ state is an almost purely closed shell state. A series of (λ,μ)=$(N,8)$ representations is a leading component of the 0_2^+ state, which indicates a well developed α+^{36}Ar(0^+) cluster structure of the state. The mixture of 0p-0h and 2p-2h configurations is not so large. The 0_3^+ state state may be of a complicated nature. A series of $(N,4)$ representations is the largest component, but many other representations are also included. The 0_3^+ state is expected to be a mixture of an α+^{36}Ar(2^+) cluster state and 2p-2h states. These points are clearly confirmed in Fig. 3, which shows the reduced width amplitudes (RWA's), $y(r)$, for the α+^{36}Ar(0^+) and α+^{36}Ar(2^+) channels. We can see a large difference of the three 0^+ states in the position and height of the outmost peak of the RWA's. These represent intuitively the degrees of surface localizations of the α cluster. The RWA of the 0_2^+ state for the α+^{36}Ar(0^+) channel has 6 nodes consistent with a 4p-4h nature. This is somewhat different from that of the α+^{12}C system. The RWA of the 2nd 0^+ state in ^{16}O has 3 nodes in spite of a 4p-4h nature [19]. This may be attributed to a difference of mixing of 2p-2h components of these states.

The 1_5^- state is dominated by a series of $(N,8)$ representations and corresponds to the α+^{36}Ar(0^+) cluster state. The main configurations of the $1_1^- \sim 1_4^-$ states are 1p-1h and 3p-3h states, but appear to contain various components of higher quanta. In the 1_1^- state the (λ,μ)=(3,2) and (9,6) representations are the main configurations. These configurations lead to strong coupling with a series of $(\lambda,\mu$=even) components, which can be viewed as an α+^{36}Ar(0^+) cluster state, while the 1_2^- state has a subtractive combination of (3,2) and (9,6) components and scarcely mixs with the α+^{36}Ar(0^+) cluster states. Such a strong mixing of 1p-1h states and α-cluster states is not observed in ^{16}O [19], because only the (2,1) and not the (3,2) of 1p-1h states is available in ^{16}O. The 1_3^- and 1_4^- states are largely (2,1) of 1p-1h states and involve an appreciable mixture of a series of $(\lambda,\mu$=odd) components, which can be viewed as α+^{36}Ar(2^+) cluster state.

The RWA's of these 1^- states for the ^{36}Ar(0^+)+α (l=1) and ^{36}Ar(2^+)+α (l=1) channels are shown in Fig. 4. We can clearly understand the mixing properties of the 1^- states. Furthermore, it may be noted that the position of the final peak of the ^{36}Ar(0^+)+α RWA of the 1_1^- state is shifted inward as compared to that of the 1_5^- state. The feature is due to a difference of components with higher quanta of the two states.

Figure 5 represents the comparison of the RWA's in the ^{36}Ar(0^+)+α channel given by the SU(3) shell model with those by the calculated α-cluster wave functions. The (12,8) J^π=0^+ state is the lowest 4p-4h state in the SU(3) model and is similar to the low-lying deformed state used in [17]. The (13,8)J^π=1^- state is expected to describe the lowest state with 5 quanta of excitations. We can clearly see a large difference in the position and height of the final peak of the RWA's. The shell model yields the S_α^2 factors of 0.040 for the 0^+ and 0.083 for the 1^- state, which are far smaller than the experiments. It is evident that the shell-model description of the α-cluster states is quite inadequate.

C. Electric transition probabilities

Matrix elements of the electric transitions can be evaluated in a microscopic way by using the knowledge of the norm kernel, and so the antisymmetric effect is properly included [5].

The calculated value of the root mean square charge radius of the ground state is 3.29 fm, which agrees well with

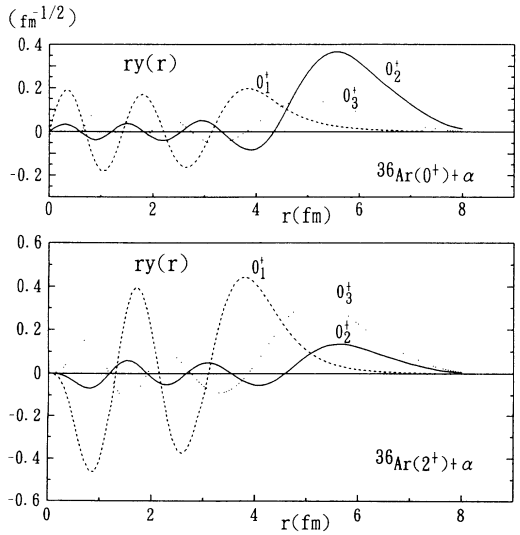

FIG. 3. The reduced width amplitudes of the three lowest 0^+ states for the ^{36}Ar(0^+)+α and ^{36}Ar(2^+)+α channels.

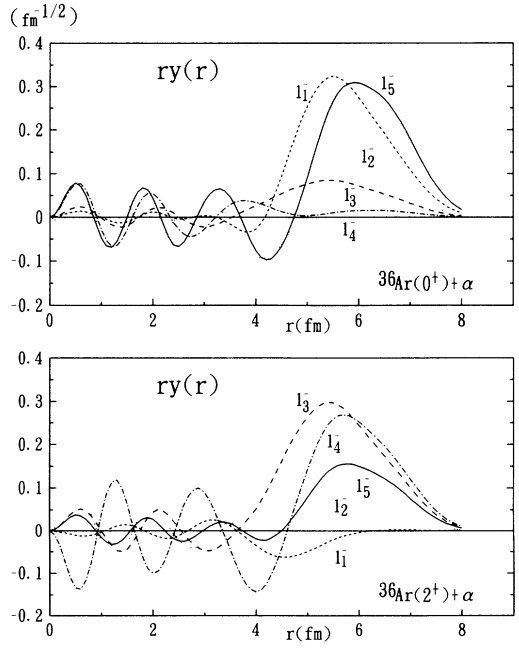

FIG. 4. The reduced width amplitudes of the five lowest 1^- states for the ^{36}Ar(0^+)+α and ^{36}Ar(2^+)+α (l = 1) channels.

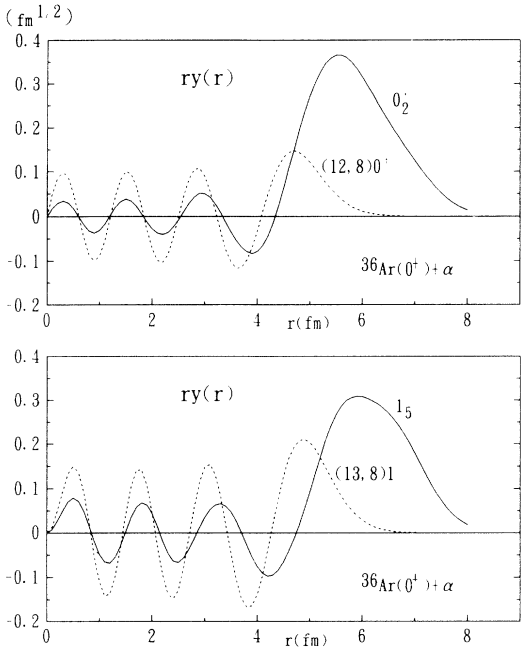

FIG. 5. Comparison of the reduced width amplitudes in the ^{36}Ar(0^+)+α channel by the SU(3) shell model with those by the present cluster model.

the observed value of 3.43 fm [21]. As for the monopole transition of the 0^+(3.35 MeV) to the ground 0^+ state, the calculated value is 1.16 fm^2 and thus slightly smaller than the experimental value of 2.53 fm^2 [21].

Calculated and observed $B(E2)$ values are summarized in Fig. 6. An additional charge $\delta e = 0.52e$ for the internal transitions of ^{36}Ar is used in order to reproduce the experimental $B(E2; 2^+ \rightarrow 0^+)$ of ^{36}Ar. A small additional charge $\delta e = 0.1e$ for the relative transitions is used, which is consistent with the value needed in the calculations of ^{44}Ti [5,15]. It is found that the in-band transitions of the α+^{36}Ar(0^+) and α+^{36}Ar(2^+) bands and also the interband transitions between them are nicely reproduced. This provides strong evidence for the existence of the α-cluster states in ^{40}Ca. The 8^+ at 10.34 MeV was reported to belong to the α+^{36}Ar(0^+) band by the recent α-transfer experiment [11]. The assumption that the 8^+ at 8.09 MeV should be associated with the α+^{36}Ar(0^+) band seems unlikely [22,23]. Because the $B(E2)$ of this level to the 6^+(6.93 MeV) is 2.5 ± 0.4 W.u., much smaller than the expected enhancement (53.8 W.u.) of the α-cluster band. In order to verify our identification, observation of the $E2$ transitions of the 8^+(10.34 MeV) level would be very useful. The $E2$ transitions of the 2^+(3.90 MeV) and 2^+(5.25 MeV) of α-cluster states to the ground 0^+ state are very small, which is a consequence of a selection rule that the transitions between the main components of the states are forbidden. The calculated values, however, are far smaller than the experimental data. Our model can only be expected to give qualitative agreement with such small values, because of complicated cancellations involved in these transitions. As for the $E2$ transitions between the negative-parity states, the calculations are in reasonable agreement with the experiments.

III. SUMMARY

In order to give a unified understanding of the structure of ^{40}Ca, we have used the microscopic α+^{36}Ar cluster model. Within this model the energy spectra, α-spectroscopic factors, and electric transition probabilities are in good overall agreement with the observed values. As a result, the existence of the parity-doublet α+^{36}Ar cluster bands has been confirmed firmly. It has been shown that the coexistence and interference of α-cluster states and shell-model states play very important roles in understanding the properties of ^{40}Ca. In the negative parity states, the mixtures of 1p-1h, 3p-3h, and α-cluster states are fairly large, which give rise to a distribution of α-cluster strength over many levels. Then the $K = 0^-$ cluster band has, on the average, smaller S_α^2 factors than the $K = 0^+$ cluster band. The α+core cluster model

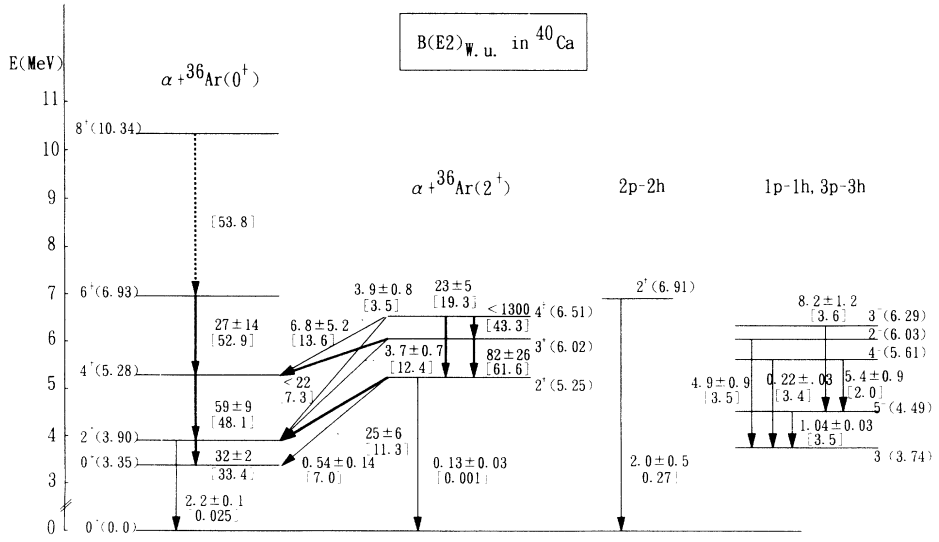

FIG. 6. Calculated and experimental $E2$ transitions of ^{40}Ca. Transitions are in W.u. The numbers are the experimental rates from Refs. [18,20,21] and the numbers in parentheses are the calculated rates. Classification of the spectra into several bands has been done according to their main components.

should certainly be equally appropriate for other nuclei in the fp-shell region as well.

ACKNOWLEDGMENTS

The authors wish to thank Professor S. Nagata for helpful discussion. This work was done as a part of the research project "Many-nucleon correlations and cluster structure in fp-shell and heavy nuclei" organized by the Yukawa Institute for Theoretical Physics, Kyoto University. The authors are greatly indebted to the members of the project. They also thank the authors of Ref. [11] for informing us of the α-spectroscopic data prior to publication.

[1] F. Michel, G. Reidemeister, and S. Ohkubo, Phys. Rev. Lett. **570**, 1215 (1986); Phys. Rev. C **37**, 292 (1988).
[2] S. Ohkubo, Phys. Rev. C **38**, 2377 (1988).
[3] S. Ohkubo and K. Umehara, Prog. Theor. Phys. **80**, 598 (1988).
[4] G. Reidemeister, S. Ohkubo, and F. Michel, Phys. Rev. C **41**, 63 (1990).
[5] T. Wada and H. Horiuchi, Phys. Rev. C **38**, 7063 (1988).
[6] A. C. Merchant, Phys. Rev. C **36**, 778 (1987); **37**, 414 (1988).
[7] K. F. Pal and R. G. Lovas, Phys. Lett. **96B**, 19 (1980).
[8] T. Yamaya, S. Oh-ami, M. Fujiwara, T. Itahashi, K. Katori, M. Tosaki, S. Kato, S. Hatori, and S. Ohkubo, Phys. Rev. C **42**, 1935 (1990).
[9] T. Yamaya, S. Oh-ami, O. Sato, M. Fujiwara, S. Hatori, T. Itahashi, K. Katori, S. Kato, M. Tosaki, and S. Ohkubo, Phys. Rev. C **41**, 2421 (1990).
[10] T. Yamaya, S. Ohkubo, S. Okabe, and M. Fujiwara, Phys. Rev. C **47**, 2389 (1993).
[11] T. Yamaya, M. Saito, M. Fujiwara, T. Itahashi, K. Katori, T. Suehiro, S. Kato, S. Hatori, and S. Ohkubo, Phys. Lett. B **306**, 1 (1993); and to be published.
[12] T. Ogawa, Y. Suzuki, and K. Ikeda, Prog. Theor. Phys. **57**, 1072 (1977); Y. Fujiwara, H. Horiuchi, K. Ikeda, M. Kamimura, K. Kato, Y. Suzuki, and E. Uegaki, Suppl. Prog. Theor. Phys. **68**, 29 (1980).
[13] Y. Goto and H. Horiuchi, Prog. Theor. Phys. **62**, 662 (1979).
[14] H. Hasegawa and S. Nagata, Prog. Theor. Phys. **45**, 1786 (1971); Y. Yamamoto, *ibid.* **52**, 471 (1974).
[15] K. Itonaga, Prog. Theor. Phys. **66**, 2103 (1981).
[16] H. T. Fortune, M. N. I. Al-Jadir, R. R. Betts, J. N. Bishop, and R. Middleton, Phys. Rev. C **19**, 756 (1979).
[17] W. J. Gerace and A. M. Green, Nucl. Phys. **A93**, 110 (1967); **A123**, 241 (1969).
[18] J. R. MacDonald, D. H. Wilkinson, and D. E. Alburger, Phys. Rev. C **3**, 219 (1971).
[19] Y. Suzuki, Prog. Theor. Phys. **56**, 111 (1976); **55**, 1751 (1976).
[20] R. Moreh, W. M. Sandefur, W. C. Sellyey, D. C. Sutton, and R. Vodhanel, Phys. Rev. C **25**, 1824 (1982).
[21] P. M. Endt, Nucl. Phys. **A521**, 1 (1990).
[22] J. J. Simpson, S. J. Wilson, P. W. Green, J. A. Kuehner, W. R. Dixon, and R. S. Storey, Phys. Rev. Lett. **35**, 23 (1975).
[23] A. M. Nathan and J. J. Kolata, Phys. Rev. C **14**, 171 (1976).